Available online at www.sciencedirect.com
SCIENCE DIRECT®
International Journal of Mass Spectrometry 226 (2003) 341–353
International Journal of Mass Spectrometry
www.elsevier.com/locate/ijms

Gas-phase solvation of Cl^-, NO_2^-, $CH_2NO_2^-$, $CH_3NO_2^-$ and $CH_3NO_4^-$ by CH_3NO_2

H. Wincel*

Institute of Physical Chemistry, Polish Academy of Sciences, 01-224 Warsaw, Poland

Received 7 January 2003; accepted 24 January 2003

Abstract

The gas-phase clustering reactions in the systems containing nitromethane were investigated with a pulsed electron-beam high-pressure mass spectrometer. The thermochemical stabilities, $\Delta H^\circ_{n-1,n}$ and $\Delta S^\circ_{n-1,n}$, of cluster ions $X^-(CH_3NO_2)_n$ ($n \leq 4$), X = Cl, NO_2, CH_2NO_2, CH_3NO_2 and CH_3NO_4, were determined. For $CH_3NO_4^-(CH_3NO_2)_n$, the binding energies are found to be significantly lower than those in corresponding cluster ions having Cl^-, NO_2^-, $CH_2NO_2^-$ and $CH_3NO_2^-$ as the core ions. This is ascribed to the dispersion of negative charge in the $CH_3NO_4^-$ core ion for which the methyl-peroxynitrate structure is postulated.

Keywords: Gas-phase equilibria; Bond enthalpies; Cluster ions; High-pressure mass spectrometer

1. Introduction

Ionic clusters can be viewed as an intermediate state of matter between the dilute gas phase and solution [1]. Laboratory studies of ionic clusters provide basic information for the elucidation of the gas-to-particle conversion processes and are of considerable importance in the context of atmospheric chemistry and a wide range of atmospheric issues [1–4].

In recent publications [5,6], we have reported the results of studies of the gas-phase clustering reactions of NO_n^+ ($n = 1, 2$) with CH_3CN and CH_3NO_2. The present work extends these studies to the negative cluster ions, $X^-(CH_3NO_2)_n$, (X = Cl, NO_2, CH_2NO_2, CH_3NO_2 and CH_3NO_4) for which the thermochemical stabilities were determined by measuring the gas-phase equilibria of the clustering reactions (1) down to the low-temperature limit at which the CH_3NO_2 vapor starts to condense on the wall of the ion source.

$$X^-(CH_3NO_2)_{n-1} + CH_3NO_2 = X^-(CH_3NO_2)_n \quad (1)$$

There is at present considerable interest in the environmental effects of NO_2^- and Cl^-, and their clusters. The NO_2^- ion plays an important role in ionosphere, stratosphere and troposphere [7,8], and Cl^- is believed to be involved in the mechanism of heterogeneous reactions on the stratospheric aerosol particles [9], leading to conversion of the relatively unreactive reservoir species such as $ClONO_2$ and HCl to more active forms, Cl_2 and HOCl, which can be photolysed by sunlight to give Cl radicals that can destroy ozone [10–12].

* Tel.: +48-22-632-32-21x3253; fax: +48-22-632-52-76.
E-mail address: wincel@ichf.edu.pl (H. Wincel).

1387-3806/03/$ – see front matter © 2003 Elsevier Science B.V. All rights reserved.
doi:10.1016/S1387-3806(03)00066-6

Here we also report an information on the clustering reactions of $CH_3NO_4^-$ which is observed under our laboratory conditions. Such species or its isomeric form may be produced in the atmosphere from methylperoxynitrate ($CH_3O_2NO_2$) which, besides HNO_3 and HNO_4, is the most important temporary reservoir of the nitrogen oxides, NO_x, in the lower stratosphere [13,14]. Its stratospheric concentration at altitude of 10 km was estimated to be $\sim 2.3 \times 10^{-12}$ [15], and lifetime ranges from 15 h up to days at middle latitude temperatures (220–226 K) [13]. The stratospheric concentration of CH_3NO_2 is much lower ($\sim 10^{-17}$ [15]), but this species is observed [16] in the stratosphere as a ligand molecule in the positive cluster ions, such as $H^+(CH_3NO_2)(H_2O)_3$ and $H^+(CH_3NO_2)(CH_3CN)(H_2O)$, and may also be observable in this region as a ligand in the anionic clusters.

A proper treatment of in situ mass spectrometric measurements of ion composition in the stratosphere and troposphere, and a more detailed understanding of the atmospheric ion chemistry require an information on the properties of the ions which atmospheric concentrations are greatly influenced by the extent of their solvation and stability. Thermodynamic data of clustering reactions contribute to the understanding of the stability and transformation of ionic clusters, and are essential in the development of aggregation phenomena involving naturally occurring ions present in the atmosphere. Formation, structure and energetics of anionic clusters is by itself an important problem of physical chemistry and chemical physics.

In a previous study [17], Sieck measured the thermochemical stabilities of the cluster ions, $Cl^-(CH_3NO_2)_n$ ($n = 1, 2$) and $NO_2^-(CH_3NO_2)$, but higher solvates have not been investigated so far. Compton et al. [18] studied the anionic nitromethane clusters using negative ion photoelectron spectroscopy from which they deduced the ion–solvent dissociation energies, $D(CH_3NO_2^-–CH_3NO_2) = 0.66 \pm 0.01$ eV and $D(CH_3NO_2)_2^-–CH_3NO_2) = 0.58 \pm 0.01$ eV.

The present work extends measurements of the thermodynamic data of $(CH_3NO_2)_n^-$, $Cl^-(CH_3NO_2)_n$ and $NO_2^-(CH_3NO_2)_n$ to larger clusters than previously reported [17,18]. The thermodynamic properties for $CH_2NO_2^-(CH_3NO_2)_n$ and $CH_3NO_4^-(CH_3NO_2)_n$ are also obtained for the first time. The present study also allows comparison of the dynamics of the $(CH_3NO_2)_n^-$ cluster decays with those of other ion clusters during diffusion to the ion source walls. Due to large dipole moment (3.46 D), the CH_3NO_2 molecule can bind the excess electron in two different ways forming dipole-bound state in which an electron is bound in the field of the dipole (mostly on the CH_3 side), and valence electronic state (mostly located on the $–NO_2$ group) [18]. Both anionic states as well as their coupling are well experimentally and theoretically documented [18–23]. In the $CH_3NO_2^-$ bare anion, the valence form is significantly more stable than the diffuse, dipole-bound state; photoelectron spectra [18] led to the electron affinity (EA) values of 12 ± 3 meV for the dipole-bound and 0.26 ± 0.8 eV for the valence states. The interaction between these two states yields a pathway for their interconversion [19] and so can open a channel of the electron loss via the dipole-bound state. This behaviour may have consequences for the dynamics of the decay of $(CH_3NO_2)_n^-$.

2. Experimental

The measurements were made with a pulsed electron-beam high-pressure mass spectrometer (PHPMS) utilising standard techniques [24]. The reactions in the ion source were initiated by the bombardment of the reagent gas by 500–1000 eV electron beam (the electron entrance pinhole was 0.1 mm in diameter). The ions produced were sampled through a slit made razor blades (15 μm × 2 mm) and magnetically mass analysed. Ion detection was provided by a channeltron equipped with a conversion dynode. Mass spectra were registered by scanning the spectrometer electromagnet with continuous electron ionisation. Thermodynamic data were obtained using an electron beam pulsed with periods of 90 μs for reaction times 1–6 ms, during which the intensity of a selected ion was collected

in a multichannel analyser as a function of its arrival time after the electron pulse. The surface of the ion source was coated with colloidal graphite to prevent charging of the surface of the ion exit slit resulted in the decrease of ion intensities in the low-temperature region. All the experimental data presented here were obtained using graphite-coated ion exit slit.

The carrier gas (N_2 or H_2) at 0.5–5 mbar was purified by passing it through a liquid N_2 cooled 4 Å molecular sieve trap. The partial pressure of CH_3NO_2 introduced into the carrier gas was varied over the 0.3–1.4 mbar range, dependent on the experimental conditions.

In the measurements of clustering reactions of Cl^-, trace amount of $CHCl_3$ were added to the carrier gas for the production of Cl^-. The Cl^- ion was probably produced by dissociative electron capture reaction:

$$e^- + CHCl_3 \rightarrow Cl^- + CHCl_2 \quad (2)$$

The reactant ion NO_2^- was mainly produced by reaction (3) on impact of CH_3NO_2 with secondary electrons degraded to energy around 0.6 eV [18,25].

$$e^- + CH_3NO_2 \rightarrow NO_2^- + CH_3 \quad (3)$$

The $CH_2NO_2^-$ may be produced by dissociative electron capture [26]

$$e^- + CH_3NO_2 \rightarrow CH_2NO_2^- + H \quad (4)$$

and also by proton transfer reactions [27].

$$O^- + CH_3NO_2 \rightarrow CH_2NO_2^- + OH \quad (5)$$

$$OH^- + CH_3NO_2 \rightarrow CH_2NO_2^- + H_2O \quad (6)$$

The O^- and OH^- anions could be the products from dissociation channels of $CH_3NO_2^-$ [21] as well as may come from a trace amount of impurities, such as O_2 and H_2O.

The formation of the parent anion, $CH_3NO_2^-$, presumably occurs via the three-body thermal electron attachment processes (7) and (8a):

$$e^- + CH_3NO_2 + M \rightleftarrows CH_3NO_2^- + M \quad (7)$$

$$e^- + 2CH_3NO_2 \rightarrow [(CH_3NO_2)_2^-]^{*-} \rightleftarrows CH_3NO_2^- + CH_3NO_2 \quad (8a)$$

The production of $CH_3NO_2^-$ in reaction channel (8a) is assumed to proceed in competition with collisional stabilisation of the excited dimer $[(CH_3NO_2)_2^-]^*$ (Channel 8b).

$$e^- + 2CH_3NO_2 \rightarrow [(CH_3NO_2)_2^-]^{*-} \xrightarrow{M} (CH_3NO_2)_2^- \quad (8b)$$

In the present experiments, the intensity of the monomer anion $CH_3NO_2^-$ was negligibly small and was observed only occasionally. This is most likely due to its short lifetime ($t < 1\,\mu s$) with respect to autodetachment [18,25]:

$$CH_3NO_2^- \rightarrow CH_3NO_2 + e^- \quad (9)$$

The equilibrium constants, $K_{n-1,n}$, were evaluated at each temperature from the expression $K_{n-1,n} = (I_n/I_{n-1})\ P$, were I_n/I_{n-1} is the measured ion intensity of the corresponding clusters at constant ratio and P is the partial pressure of CH_3NO_2. The thermodynamic values, $\Delta H^\circ_{n-1,n}$ and $\Delta S^\circ_{n-1,n}$, were derived from the temperature studies of the equilibrium constants using the van't Hoff equation $K_{n-1,n} = (\Delta H^\circ_{n-1,n}/RT) + (\Delta S^\circ_{n-1,n}/R)$. The measured $K_{n-1,n}$ for all clustering reactions studied were found to be independent of the change of partial pressures of CH_3NO_2 in the range 0.5–1.4 mbar. The bending over in the van't Hoff plots was not observed in the present experiments. This suggests that the collision induced dissociation of cluster ions extracted through the ion slit was negligible.

The chemicals, N_2 (99.999%), CH_3NO_2 (99.9%) and CD_3NO_2 (99% atom D) were purchased from commercial sources. The CH_3NO_2 sample used was checked by GC/MS analysis which showed no impurities.

3. Results and discussion

3.1. General description of reactions

Typical mass spectra showing the negative ions produced in the CH_3NO_2/N_2 mixture are presented in Fig. 1. The cluster ions observed include

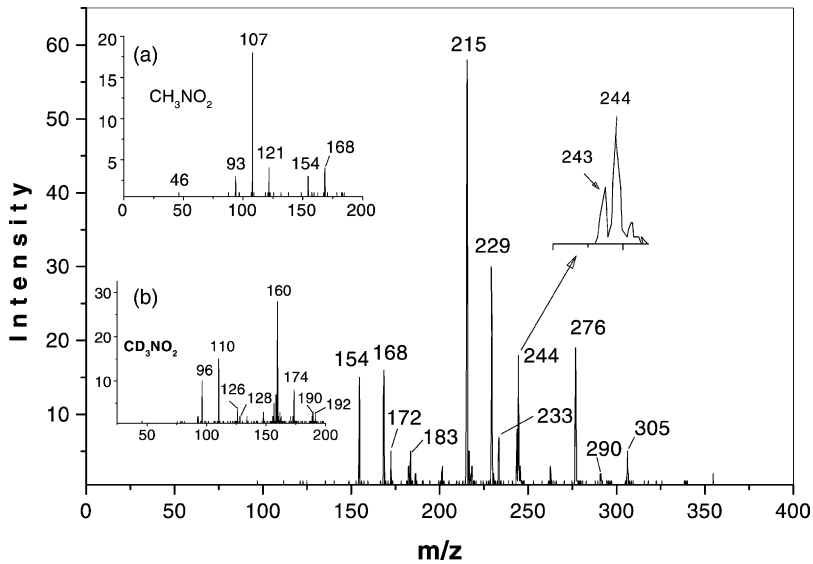

Fig. 1. Anion mass spectrum of the 26% CH_3NO_2/NO_2 gas mixture recorded at source pressure of 3.8 mbar and $T = 265$ K. The insets show partial mass spectra of the mixture: (a) 26% CH_3NO_2/N_2 at 3.8 mbar and $T = 301$ K; (b) 29%CD_3NO_2/N_2 at 3.5 mbar and $T = 340$ K. The peaks at *m/z* 46, 107, 168, 229, 290 assigned to $NO_2^-(CH_3NO_2)_n$ (n = 0–4); *m/z* 93, 154, 215, 276—$CH_3NO_4^-(CH_3NO_2)_n$ (n = 0–3); *m/z* 121, 182, 243—$CH_2NO_2^-(CH_3NO_2)_n$ (n = 1–3); *m/z* 183, 244, 305—$CH_3NO_2^-(CH_3NO_2)_n$ (n = 2–4); *m/z* 110, 174—$NO_2^-(CD_3NO_2)_n$ (n = 1, 2); *m/z* 96, 160—$CD_3NO_4^-(CD_3NO_2)_n$ (n = 0, 1); *m/z* 126, 190—$CD_2NO_2^-(CD_3NO_2)_n$ (n = 1, 2); *m/z* 128, 192—$CD_3NO_4^-(CD_3NO_2)_n$ (n = 1, 2).

$NO_2^-(CH_3NO_2)_n$, $CH_2NO_2^-(CH_3NO_2)_n$, $(CH_3NO_2)_n^-$ and a series of ions at *m/z* 93, 154, 215 and 276, which could correspond to $A^-(CH_3NO_2)_n$, where A^- stands for the core anion of *m/z* 93. The ions with *m/z* 172 and 233 may be assigned to $A^-(CH_3NO_2)_n{\cdot}H_2O$ with $n = 1$ and 2. The identification of these series of cluster ions is confirmed by the correct isotope shift seen when CD_3NO_2 is used (see insets in a and b, Fig. 1). In the case of CD_3NO_2, the peak of *m/z* 93 shifts to 96. This suggests that the core ion A^- (*m/z* 93) may have the formal structure $CH_3NO_4^-$. The fact that the same ions, $CH_3NO_4^-$ and its analogue $CD_3NO_4^-$, are found to be formed in the mixtures containing nitromethane (CH_3NO_2 and CD_3NO_2, respectively) obtained from different suppliers can be considered as an indication that these species may not be due to the eventual impurities content in the nitromethane samples but could be produced in the reactions occurring in the ion source. The following reactions may be responsible for the formation of $CH_3NO_4^-$.

One possibility is the three-body reaction (10):

$$NO_2^- + CH_3O_2 + M \rightarrow CH_3NO_4^- + M \quad (M : \text{thirdbody}) \qquad (10)$$

This reaction is analogous to that observed for the neutral reactants, NO_2 and CH_3O_2, leading to the production of methyl-peroxynitrate in the lower atmosphere [13,14]. Since this compound is thermally unstable under the normal conditions, it seems unlikely that it could be introduced into the ion source as an impurity of the nitromethane samples (CH_3NO_2 or CD_3NO_2). Also, the methylperoxy radical, CH_3O_2, may undergo significant thermal decomposition on metal surfaces [28].

In the present experiments, CH_3O_2 could be produced in the ion source by the reaction:

$$CH_3 + O_2 + M \rightleftarrows CH_3O_2 + M \qquad (11)$$

The potential-energy surface calculated [29] for the reaction $CH_3 + O_2$ predicts that CH_3 adds to O_2

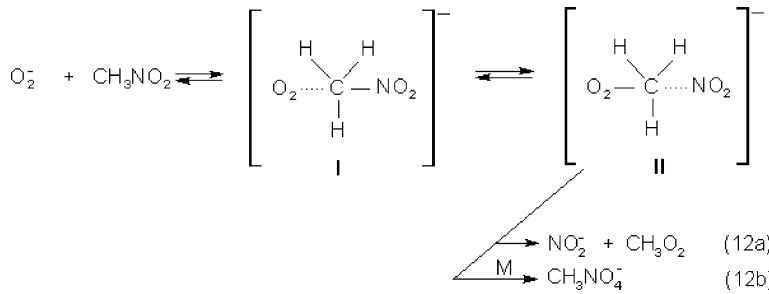

Scheme 1.

without any energetic barrier. The CH_3 species, needed for the CH_3O_2 production, may be generated from nitromethane during the electron irradiation ($e^- + CH_3NO_2 \rightarrow NO_2^{\pm} + CH_3$), while O_2 could be a minor (about 1 ppm) impurity present in the N_2 carrier gas. It is worthy to note that aside water, O_2 is a common impurity of the carrier gases, and effects of trace levels of O_2 on the formation of the oxygen-derived unexpected ions in the PHPMS studies have been reported in several papers (for reviews, see [30]). However, in a view of our previous discussion [31], the gaseous concentration of CH_3 resulting from the electron irradiation of CH_3NO_2 should be about three orders of magnitude lower than that of CH_3NO_2. Thus, due to expected very low concentrations of both reactants involved in the reaction (11), the contribution of this pathway to the production of CH_3O_2 (and as a consequence of this also $CH_3O_4^-$) will be more or less negligible under the present experiments.

Another possibility for the formation of $CH_3NO_4^-$ is the direct termolecular addition $[O_2 + CH_3NO_2]^- + M$. When a small amount (~0.2 mbar) of O_2 was intentionally added to the CH_3NO_2/N_2 reaction system at a total pressure of 1.1 mbar (at 350 K), the abundances of $NO_2^-(CH_3NO_2)_n$ ($n = 1, 2$), $CH_3NO_4^-(CH_3NO_2)_n$ ($n = 0, 1$) and $CH_2NO_2^-(CH_3NO_2)_n$ ($n = 1, 2$) were found to increase by a factor of about 1.4. This observation suggests that oxygen (as O_2^- or O_2) is involved in the reaction mechanisms leading to the formation of the core ions for these clusters. (Note that in none of the experiments reported in this paper, the presence of O_2^- have been observed, presumably because it reacts rapidly enough to be below the limit of detectability). While the increase of $CH_2NO_2^-(CH_3NO_2)_n$ ($n = 1, 2$) observed after addition of O_2 may be due to the production of O^- (from O_2), which in reaction (5) leads to the formation of the $CH_2NO_2^-$ core anion, the enhancement in intensities of $NO_2^-(CH_3NO_2)_n$ ($n = 1, 2$) and $CH_3NO_4^-(CH_3NO_2)_n$ ($n = 0, 1$) may be attributed to the production of NO_2^- and $CH_3NO_4^-$ by the reaction mechanism proposed in Scheme 1 involving nucleophilic attack of O_2^- on the carbon atom of CH_3NO_2. The anion radical, O_2^-, in aprotic solvents is known to be a strong nucleophile in gas-phase ion–molecule reactions with a variety of organic compounds [32–34].

The S_N2-type pathway (12a) is exothermic by 11.1 kcal/mol [35], and is assumed to occur through the formation of an intermediate ion–neutral complex, **I**, which rearranges to **II**, for NO_2^- displacement reaction. As the electron affinity $EA(NO_2) = 2.30$ eV (if not stated otherwise, all thermochemical data have been taken from [35a]) is higher than $EA(CH_3OO) = 1.14$ eV (for a value of ΔH_f (CH_3OO) = 6.2 kcal/mol, see [35b]), the formation of the NO_2^- ion product is favoured. The $CH_3NO_4^-$ ion may be considered as the collisionally stabilised ion–dipole intermediate complex, **II**, which might rearrange to the methyl-peroxynitrate structure, $CH_3O_2NO_2^-$. The complete answer on the structure of $CH_3NO_4^-$ awaits further experiments, such as mass selected ions and the MI/CA techniques as well as the computational study of the isomeric structures of $CH_3NO_4^-$.

The proposed mechanism (Scheme 1) is consistent with the observed temperature dependence measurements presented in Fig. 2, which show that with a

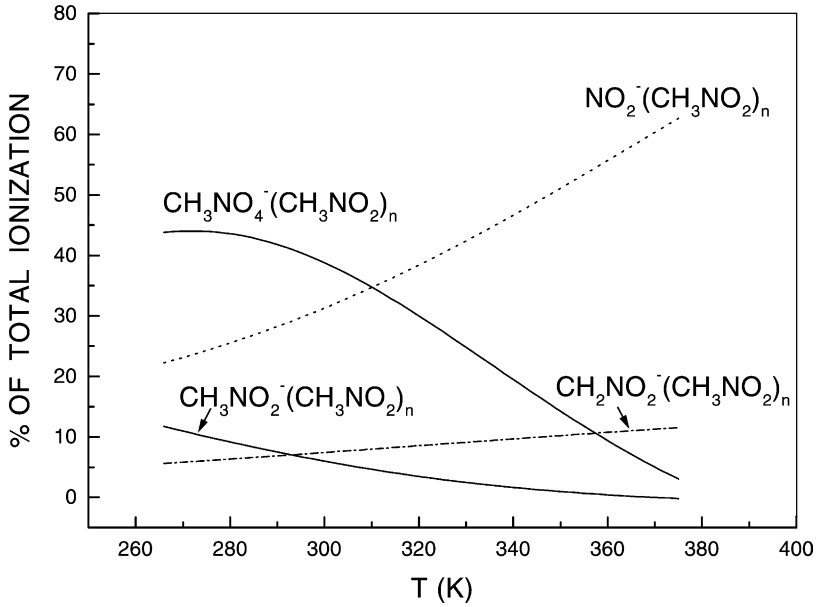

Fig. 2. Temperature dependence of the normalised total intensities of the cluster ions observed in the mass spectra of 24% CH_3NO_2/N_2 at source pressure of 3.6 mbar.

decrease of the ion source temperature, the total intensity of $NO_2^-(CH_3NO_2)_n$ series decreases accompanied by increase that of $CH_3NO_4^-(CH_3NO_2)_n$, which become the dominant products at the low-temperature-end of the experiments.

Finally, we cannot rule out the possibility that CH_3O_2 and $CH_3O_4^-$ may be formed by the reactions on the ion source surface. Such reactions have been suggested as responsible for the appearance of the unexpected ions in high-pressure electron-capture mass spectra of many nitrocompounds [30].

Unfortunately, owing to experimental limitations, we are left with some uncertainty with regard to the origination of $CH_3NO_4^-$. Nevertheless, the examination of the clustering reactions of this anion together with other anionic species seems to be of interest.

Let us now turn to the behaviour of $(CH_3NO_2)_n^-$ presented in Fig. 2 which shows a clear trend in efficiency of the formation of these clusters with decrease of temperature. This trend is analogous to that of $CH_3NO_4^-(CH_3NO_2)_n$ and can be accounted for by a consideration of the lifetime of the collision complex $[(CH_3NO_2)_2^-]^*$ involved in reaction (8). As already mentioned, this complex can be destroyed by fragmentation to the monomer species or can be stabilised by subsequent collision. With a decrease of temperature, the lifetime of $[(CH_3NO_2)_2^-]^*$ increases and efficiency of the complex stabilisation is expected to increase resulting in the increase of the forward rate leading to the formation of larger cluster ions $(CH_3NO_2)_n^-$.

In contrast, the series of the cluster ions $CH_2NO_2^-(CH_3NO_2)_n$ is seen to decrease with a decrease of temperature. As in the case of $(CH_3NO_2)_n^-$, this is presumably a consequence of influence of temperature on the internal energy of the excited $(CH_3NO_2^-)^*$ anion (or other species) produced by the electron attachment channel, which leads directly to the $CH_2NO_2^-$ core ion (Reaction 4) or via its precursors, such as O^- and OH^- (Reactions 5 and 6).

3.2. Equilibrium measurements for clustering reactions

The results described above provide a basis for the observation of the corresponding equilibria for

Table 1
Thermochemical data, $\Delta H^{\circ}_{n-1,n}$ (kcal/mol) and $\Delta S^{\circ}_{n-1,n}$ (cal/mol K)[a], for the gas-phase clustering reactions: $Cl^-(CH_3NO_2)_{n-1} + CH_3NO_2 \rightleftarrows Cl^-(CH_3NO_2)_n$ and $NO_2^-(CH_3NO_2)_{n-1} + CH_3NO_2 \rightleftarrows NO_2^-(CH_3NO_2)_n$

n	Cl^-		NO_2^-	
	$-\Delta H^{\circ}_{n-1,n}$	$-\Delta S^{\circ}_{n-1,n}$	$-\Delta H^{\circ}_{n-1,n}$	$-\Delta S^{\circ}_{n-1,n}$
1	15.6 ± 0.6	21.4 ± 3	14.5 ± 0.5	22.5 ± 2
	16.7[b]	17.1[b]	14.3[b]	15.5[b]
2	13.0 ± 0.5	24.6 ± 3	12.4 ± 0.5	23.4 ± 3
	13.1[b]	18.3[b]		
3	11.1 ± 0.5	24.7 ± 3	11.3 ± 0.8	26.8 ± 3
4	9.6 ± 1	23 ± 4	9.7 ± 0.3	27.2 ± 3

Results given to the temperature of the van't Hoff plot. However, since the ΔS° dependence upon the temperature is small, ΔS° values are approximately equal to those at 298 K.
[a] Standard state 1 atm.
[b] Ref. [17].

the clustering reactions of the NO_2^-, $CH_2NO_2^-$, $CH_3NO_2^-$ and $CH_3NO_4^-$ anions with CH_3NO_2.

Fig. 3 shows, as an example, the temporal profiles of $CH_3NO_2^-(CH_3NO_2)_n$ and $CH_3NO_4^-(CH_3NO_2)_n$ observed in the 26% CH_3NO_2/N_2 gas mixture. Approach to equilibrium for reactions (1) were observed ~300–400 μs after the electron pulse, depending on the experimental conditions. The temperature dependence of the measured equilibrium constants for these reactions are displayed in the van't Hoff plots of Fig. 4. The lower limits of temperatures for the measurement of the equilibrium constants correspond to the start of the condensation of CH_3NO_2. The thermodynamic data derived from such plots for the all systems studied are summarised in Tables 1 and 2. Some previous data from other laboratories are also included in the tables for comparison. The reported $\Delta H^{\circ}_{n-1,n}$ and $\Delta S^{\circ}_{n-1,n}$ values are the averages of at least three measurements, each obtained from a weighted least-squares fit of the van't Hoff plots. The error limits show the statistical fluctuations; the absolute error from an unknown true value may be greater. The slow decrease of the $-\Delta H^{\circ}_{n-1,n}$ values with n (Fig. 5) suggests that the core ion–ligand interaction involved in the cluster ions is mainly electrostatic in nature. Some irregularities in the $-\Delta H^{\circ}_{n-1,n}$ change sequence are within the range of the experimental uncertainty (Fig. 5, and Tables 1 and 2) and cannot be taken into consideration for the shell formation in these clusters. It is logical to expect that the ion–ligand bond formation in these species occurs through the interaction of methyl group of CH_3NO_2 with the negative charge site of anions. The results in Table 1 demonstrate that the binding energy for Cl^-–CH_3NO_2 is slightly stronger than that of NO_2^-–CH_3NO_2. This is probably due to the higher density of charge on Cl^- compared to NO_2^- in which the negative charge is located upon the O atoms.

The $-\Delta H^{\circ}_{n-1,n}$ values (Table 2) for $CH_3NO_4^-(CH_3NO_2)_n$ indicate that these cluster ions are less stable than the corresponding of $CH_3NO_2^-(CH_3NO_2)_n$. This difference can be attributed to the lower charge

Table 2
Thermochemical data, ΔH° (kcal/mol) and ΔS° (cal/mol K)[a], for the gas-phase clustering reactions: $CH_2NO_2^-(CH_3NO_2)_{n-1} + CH_3NO_2 \rightleftarrows CH_2NO_2^-(CH_3NO_2)_n$, $CH_3NO_2^-(CH_3NO_2)_{n-1} + CH_3NO_2 \rightleftarrows CH_3NO_2^-(CH_3NO_2)_n$ and $CH_3NO_4^-(CH_3NO_2)_{n-1} + CH_3NO_2 \rightleftarrows CH_3NO_4^-(CH_3NO_2)_n$

n	$CH_2NO_2^-$		$CH_3NO_2^-$		$CH_3NO_4^-$	
	$-\Delta H^{\circ}_{n-1,n}$	$-\Delta S^{\circ}_{n-1,n}$	$-\Delta H^{\circ}_{n-1,n}$	$-\Delta S^{\circ}_{n-1,n}$	$-\Delta H^{\circ}_{n-1,n}$	$-\Delta S^{\circ}_{n-1,n}$
1	15.9 ± 0.5	25 ± 2	15.18 ± 0.2[b]		13.0 ± 0.8	22 ± 3
2	13.3 ± 0.7	25 ± 2	12.80 ± 0.3	23 ± 1	10.9 ± 0.6	24 ± 3
			13.34 ± 0.2[b]			
3	12.6 ± 0.5	32 ± 2	10.40 ± 0.5	22 ± 2	9.5 ± 0.9	24 ± 4
4	11.4 ± 0.2	33 ± 2	8.40 ± 0.2	20 ± 2	6	~18

Results given to the temperature of the van't Hoff plot. However, since the ΔS° dependence upon the temperature is small, ΔS° values are approximately equal to those at 298 K.
[a] Standard state 1 atm.
[b] Ref. [18].

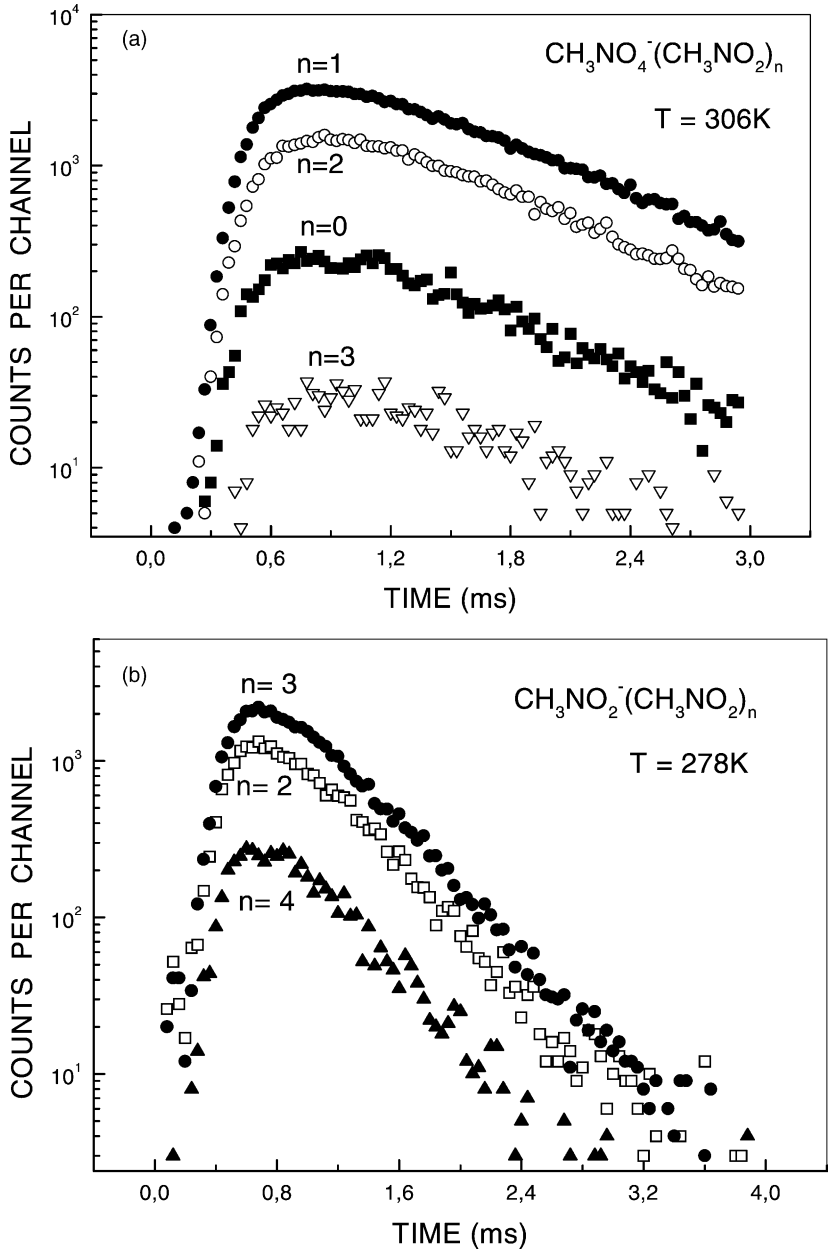

Fig. 3. The temporal profiles of the cluster ions: (a) $CH_3NO_4^-(CH_3NO_2)_n$ ($n = 0$–3) and (b) $CH_3NO_2^-(CH_3NO_2)_n$ ($n = 2$–4) observed in the 26% CH_3NO_2/N_2 mixture at indicated temperatures and a source pressure of 3.8 mbar. Electron pulse width, 90 μs; channel dwell time: (a) 30 μs; (b) 40 μs; energy of incident electrons = 600 eV. At 4 ms, a short (90 μs) pulse (−50 V) is applied to the repeller electrode in order to annihilate all ions produced in the ion source.

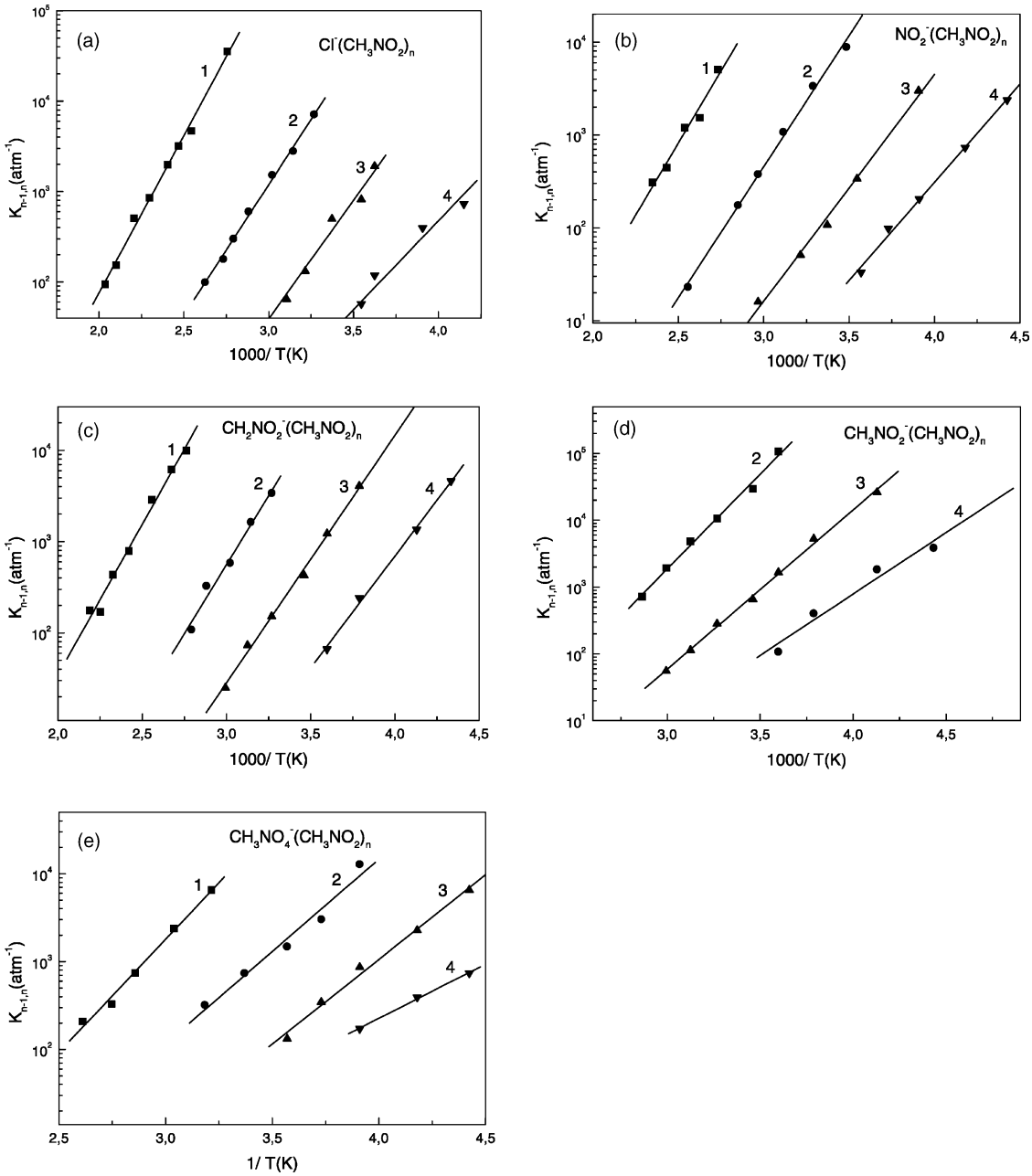

Fig. 4. van't Hoff plots for the equilibria $X^-(CH_3NO_2)_{n-1} + CH_3NO_2 \rightleftarrows X^-(CH_3NO_2)_n$, X = (a) Cl; (b) NO_2; (c) CH_2NO_2; (d) CH_3NO_2; (e) CH_3NO_4. The numbers shown in the figures correspond to the value of *n*.

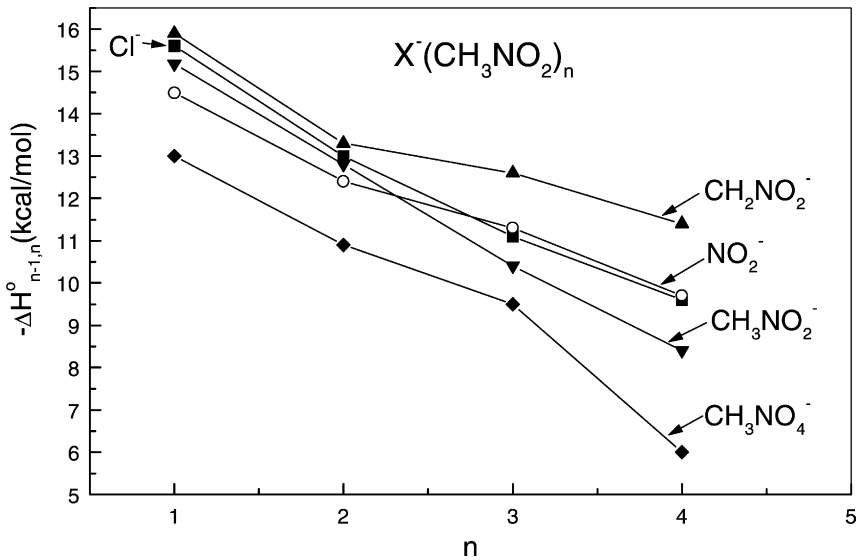

Fig. 5. The n dependence of the bond energies—$\Delta H^{\circ}_{n-1,n}$ (kcal/mol) of the cluster ions: $Cl^-(CH_3NO_2)_n$ (■); $NO_2^-(CH_3NO_2)_n$ (○); $CH_2NO_2^-(CH_3NO_2)_n$ (▲); $CH_3NO_2^-(CH_3NO_2)_n$ (▼) (for $n = 1$, see ref. [18]); $CH_3NO_4^-(CH_3NO_2)_n$ (◆).

density localised on the negative sites of the core ion $CH_3NO_4^-$. This is in keeping with the possible methyl-peroxynitrate structure for this species.

In the case of $CH_2NO_2^-(CH_3NO_2)_n$ and $CH_3NO_2^-(CH_3NO_2)_n$, the $-\Delta H^{\circ}_{n-1,n}$ values for $n = 1$ and 2 are nearly the same but at higher n the solvation of $CH_3NO_2^-$ becomes less favourable than $CH_2NO_2^-$. Furthermore, the $-\Delta S^{\circ}_{n-1,n}$ values of $CH_2NO_2^-\cdot(CH_3NO_2)_n$ are found (Table 2) to be considerably larger than those of corresponding $CH_3NO_2^-(CH_3NO_2)_n$. These results may reflect the difference in the structures of the cluster ions. While the first two additions to both core ions are thought to involve attack of methyl group of CH_3NO_2 upon O atoms of $CH_2NO_2^-$ and $CH_3NO_2^-$, the next two ligands in $CH_2NO_2^-(CH_3NO_2)_n$ may be expected to form a structure of type **IIIa**, in which C···H hydrogen bond formation is probable, since the C atom of the $CH_2NO_2^-$ core ion must be considered as bearing some degree of negative charge; another possibility is a hydrogen bonded structure such as **IIIb**.

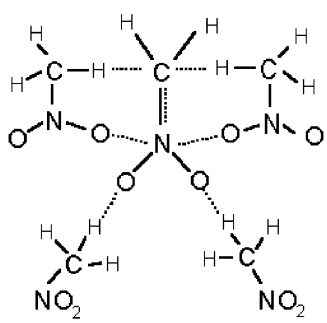

IIIa

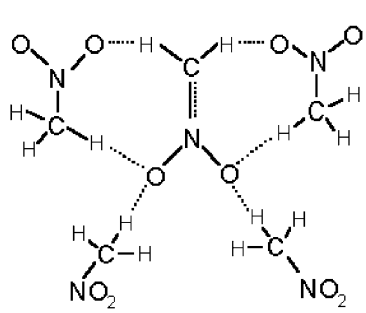

IIIb

In such structures, a partial C=N double bond in $CH_2NO_2^-$ as well as an intracluster hydrogen bonding could preclude rotation around the C–N bond and the

bending motions of the bonds between $CH_2NO_2^-$ and CH_3NO_2 providing rigidity of these structures manifested by the $-\Delta S^\circ_{n-1,n}$ values.

Since the $-\Delta S^\circ_{n-1,n}$ values for $CH_3NO_2^-(CH_3NO_2)_n$ are found to be relatively smaller (Table 2), the CH_3NO_2 ligands in these clusters must have more freedoms of motion (more flexible) than those in $CH_2NO_2^-(CH_3NO_2)_n$. The photoelectron spectra of $CH_3NO_2^-(CH_3NO_2)_n$ ($n = 0-2$) provided an experimental indication that the excess of charge in these clusters is localised on one CH_3NO_2 molecule, and the $CH_3NO_2^-$ anions produced by evaporation from $(CH_3NO_2)_2^-$ and larger clusters are in valence states [18]. In this respect, the $(CH_3NO_2)_n^-$ anions should be more appropriately represented as $CH_3NO_2^-(CH_3NO_2)_n$. Taking into consideration all these results and assuming that in the $CH_3NO_2^-$ valence core anion the excess electron occupation is largely associated with $-NO_2$ group, it seems reasonable to propose that the third and fourth ligand additions in $CH_3NO_2^-(CH_3NO_2)_n$ occur to the oxygen atoms of the core ion, as shown in structure **IVa**.

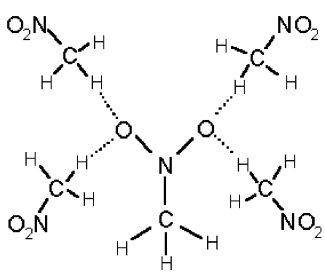

IVa

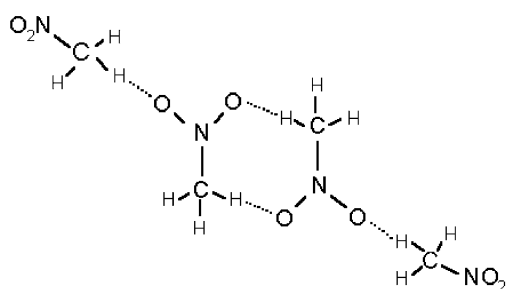

IVb

The isomeric structure **IVb** is also possible and may be formed by attachment of the CH_3NO_2 neutrals to the oxygen atom of the cyclic dimer, $(CH_3NO_2)_2^-$. The CNDO calculations [36] on the CH_3NO_2 dimer predict that the hydrogen bonded cyclic structure is the most stable. In the present case, the ionised form of such structure can arise from reaction (8b).

From Fig. 6 it is seen that the loss of $CH_3NO_2^-(CH_3NO_2)_2$ is remarkably more rapid than those of other clusters. A similar differences in the dynamics of decay between these series of cluster ions have been also observed for the corresponding smaller and larger clusters in the measurements performed under the same experimental conditions and gas phase composition in the temperature range of 265–348 K. (Note that for non-reactive ion, the loss of intensity with time represents the decay due to ion diffusion to the walls of the ion source.)

These observations imply that in the case of $CH_3NO_2^-(CH_3NO_2)_n$ some reaction superimposes on their diffusive loss. Although we cannot exclude the possibility that the reactive disappearance of these clusters is due to some ion–molecule reaction with eventual impurities, but it seems likely that the observed behaviour in relatively rapid decay of these species is a consequence of the dual anionic character of $CH_3NO_2^-$. As discussed in the Introduction, the interconversion between the dipole and valence states yields a pathway to electron loss. Thus, one may speculate that this pathway can also open an avenue to the intracluster transfer for an excess electron what in consequence could led to more efficient mechanism of the loss of $CH_3NO_2^-(CH_3NO_2)_n$ due to the intracluster or/and intramolecular electron transfer during "diffusion" of these clusters to the walls of the ion source.

Since the ratios of the rate constants of the $CH_3NO_2^-(CH_3NO_2)_n$ decay to those of other cluster ions, $X^-(CH_3NO_2)_n$, X = Cl, NO_2, CH_2NO_2 and CH_3NO_4, measured at different temperatures from the slopes of the plots of log(Ion signal) versus time, such as shown in Fig. 6, are found to yield within the experimental error the same value of 2.4, contribution of the reactive loss of $CH_3NO_2^-(CH_3NO_2)_n$

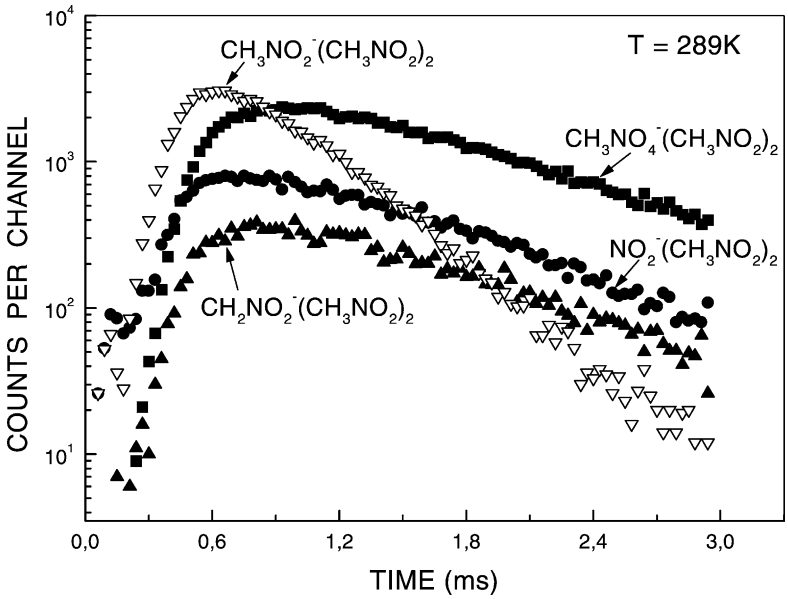

Fig. 6. Ion intensity of the indicated ion clusters as a function of time after 90-μs electron pulse observed in the 26% CH_3NO_2/N_2 mixture at a constant source temperature of 289 K and a constant total pressure of 3.8 mbar.

due to the shifting in the equilibrium sequence, $CH_3NO_2^-(CH_3NO_2)_n \rightarrow \cdots \rightarrow CH_3NO_2^- \rightarrow CH_3NO_2 + e^-$, is expected to be negligible.

4. Conclusions

In this work, gas-phase clustering reactions between $CH_3NO_4^-$ and five anions, Cl^-, NO_2^-, $CH_2NO_2^-$, $CH_3NO_2^-$ and $CH_3NO_4^-$, have been investigated down to the condensation point of the sample vapour. The addition reactions with $CH_3NO_2^-$ and $CH_3NO_4^-$ show an increasing efficiency with decreasing temperature. This trend is consistent with the concept of collision-complex lifetimes. A series of $CH_3NO_4^-(CH_3NO_2)_n$ becomes the dominant product ions at the low-temperature-end of the experiments.

The thermochemical data obtained in the present and previous studies [17] show that the bond energies $D(X^-–CH_3NO_2)$ for X = Cl and NO_2 are close to the corresponding values $D(X^-–H_2O)$. The fact that the stratospheric concentration of water ($\sim 10^{-6}$ [37]) is much higher than that of CH_3NO_2 ($\sim 10^{-17}$ [15]), the possibility for observation of $Cl^-(CH_3NO_2)_n$ and $NO_2^-(CH_3NO_2)_n$ in the stratosphere seems to be very little probable.

References

[1] A.W. Castleman Jr., Environ. Sci. Technol. 22 (1988) 1265.
[2] W. A Castleman Jr., K.H. Bowen Jr., J. Phys. Chem. 100 (1996) 12911.
[3] G. Niedner-Schatteburg, V.E. Bondybey, Chem. Rev. 100 (2000) 4059.
[4] R.S. Mac Taylor, A.W. Castleman Jr., J. Atmos. Chem. 36 (2000) 23.
[5] H. Wincel, Chem. Phys. Lett. 292 (1998) 193.
[6] H. Wincel, Int. J. Mass Spectrom. 203 (2000) 93.
[7] E.E. Ferguson, F. Arnold, Acct. Chem. Res. 14 (1981) 327.
[8] D. Smith, P. Spanel, Mass Spectrom. Rev. 14 (1995) 255.
[9] B.J. Gertner, J.T. Hynes, Science 271 (1996) 1563.
[10] C.R. Webster, R.D. May, D.W. Toohey, L.M. Avallone, J.G. Anderson, P. Newman, L. Lait, M.R. Schoeberl, J.W. Elkins, K.R. Chan, Science 261 (1993) 1130.
[11] O. Toon, E. Browell, B. Gary, L. Lait, J. Livingston, P. Newman, R. Pueschell, P. Russell, M. Schoeberl, G. Toon, W. Traub, F.P.J. Valero, H. Sekirk, J. Jordan, Science 261 (1993) 1136.
[12] D.C. Clary, L. Wang, J. Chem. Soc. Faraday Discuss. 93 (1997) 2763.

[13] A.G. KraabØl, P. Konopka, F. Stordal, H. Schlager, Atmos. Environ. 34 (2000) 3939.
[14] A.G. KraabØl, F. Stordal, Atmos. Environ. 34 (2000) 3951.
[15] R.C. Costen, G.M. Tennille, J.S. Levine, J. Geophys. Res. 93 (1988) 941.
[16] E. Arijs, Ann. Geophys. 1 (1983) 149.
[17] L.W. Sieck, J. Phys. Chem. 89 (1985) 5552.
[18] R.N. Compton, H.S. Carman Jr., C. Desfrancois, H. Abdoul-Carmine, J.P. Schermann, J.H. Hendricks, S.A. Lyapustina, K.H. Bowen, J. Chem. Phys. 105 (1996) 3472.
[19] F. Lecomte, S. Carles, C. Desfrancois, M.A. Johnson, J. Chem. Phys. 113 (2000) 10973.
[20] I.C. Walker, M.A.D. Fluendy, Int. J. Mass Spectrom. 205 (2001) 171.
[21] G.L. Gutsev, R.J. Barlett, J. Chem. Phys. 105 (1996) 8785.
[22] J.M. Weber, W.H. Robertson, M.A. Johnson, J. Chem. Phys. 115 (2001) 10718.
[23] T. Sommerfeld, Phys. Chem. Chem. Phys. 4 (2002) 2511.
[24] H. Wincel, Int. J. Mass Spectrom. Ion Processes 175 (1998) 283.
[25] J.A. Stockdale, F.J. Davis, R.N. Compton, C.E. Klots, J. Phys. Chem. 60 (1974) 4279.
[26] E.C.M. Chen, N. Welk, E.S. Chen, W.E. Wentworth, J. Phys. Chem. A 103 (1999) 9072.
[27] J.J. Grabowski, S.J. Melly, Int. J. Mass Spectrom. Ion Processes 81 (1987) 147.
[28] C.A. Schalley, R. Wesendrup, D. Schröder, T. Weiske, H. Schwarz, J. Am. Chem. Soc. 117 (1995) 7711.
[29] S.P. Walch, Chem. Phys. Lett. 215 (1993) 81.
[30] W.B. Knighton, L.J. Sears, E.P. Grimsrud, Mass Spectrom. Rev. 14 (1995) 327.
[31] Z. Łuczyński, H. Wincel, Int. J. Radiat. Phys. Chem. 7 (1975) 705.
[32] D.T. Sawuer, J.S. Valentine, Acc. Chem. Res. 14 (1981) 393.
[33] R.N. McDonald, A.K. Chowdhury, J. Am. Chem. Soc. 107 (1985) 4123.
[34] C.A. Mayhew, R. Peverall, P. Watts, Int. J. Mass Spectrom. Ion Processes 125 (1993) 81.
[35] (a) S.G. Lias, J.E. Bartmess, J.F. Liebman, J.L. Holmes, R.D. Levin, W.G. Mallard, J. Phys. Chem. Ref. Data (Suppl. 1) (1988).;
(b) Ch.A. Schalley, D. Schröder, H. Schwarz, K. Möbus, G. Boche, Chem. Ber. 130 (1997) 1085.
[36] B. Brakaspathy, S. Singh, J. Mol. Struct. (Theochem.) 164 (1988) 319.
[37] P.J. Crutzen, F. Arnold, Nature 324 (1986) 651.